

RESEARCH ARTICLE

10.1002/2016JD026025

Key Points:

- Atmospheric dynamics in the Caribbean
- SST over the Caribbean Sea is examined as kinetic energy source for the CLLJ
- Impact of meridional SST gradient on the vertical structure of CLLJ

Correspondence to:

T. Maldonado,
tito.maldonado@ucr.ac.cr

Citation:

Maldonado, T., A. Rutgersson, R. Caballero, F. S. R. Pausata, E. Alfaro, and J. Amador (2017), The role of the meridional sea surface temperature gradient in controlling the Caribbean low-level jet, *J. Geophys. Res. Atmos.*, 122, doi:10.1002/2016JD026025.

Received 29 SEP 2016

Accepted 29 MAY 2017

Accepted article online 31 MAY 2017

The role of the meridional sea surface temperature gradient in controlling the Caribbean low-level jet

Tito Maldonado^{1,2,3,4} , Anna Rutgersson² , Rodrigo Caballero⁵ , Francesco S. R. Pausata^{5,6} , Eric Alfaro^{3,7,8} , and Jorge Amador^{3,8} 

¹Centre for Natural Disaster Science, Uppsala University, Uppsala, Sweden, ²Department of Earth Sciences, Uppsala University, Uppsala, Sweden, ³Center for Geophysical Research (CIGEFI), University of Costa Rica, San Pedro, Costa Rica, ⁴Now at San Pedro, Costa Rica, ⁵Department of Meteorology and Bolin Centre for Climate Research, Stockholm University, Stockholm, Sweden, ⁶Department of Earth and Atmospheric Sciences, University of Quebec in Montreal, Montreal, Quebec, Canada, ⁷Center for Research in Marine Sciences and Limnology (CIMAR), University of Costa Rica, San Pedro, Costa Rica, ⁸School of Physics, University of Costa Rica, San Pedro, Costa Rica

Abstract The Caribbean low-level jet (CLLJ) is an important modulator of regional climate, especially precipitation, in the Caribbean and Central America. Previous work has inferred, due to their semiannual cycle, an association between CLLJ strength and meridional sea surface temperature (SST) gradients in the Caribbean Sea, suggesting that the SST gradients may control the intensity and vertical shear of the CLLJ. In addition, both the horizontal and vertical structure of the jet have been related to topographic effects via interaction with the mountains in Northern South America (NSA), including funneling effects and changes in the meridional geopotential gradient. Here we test these hypotheses, using an atmospheric general circulation model to perform a set of sensitivity experiments to examine the impact of both SST gradients and topography on the CLLJ. In one sensitivity experiment, we remove the meridional SST gradient over the Caribbean Sea and in the other, we flatten the mountains over NSA. Our results show that the SST gradient and topography have little or no impact on the jet intensity, vertical, and horizontal wind shears, contrary to previous works. However, our findings do not discount a possible one-way coupling between the SST and the wind over the Caribbean Sea through friction force. We also examined an alternative approach based on barotropic instability to understand the CLLJ intensity, vertical, and horizontal wind shears. Our results show that the current hypothesis about the CLLJ must be reviewed in order to fully understand the atmospheric dynamics governing the Caribbean region.

1. Introduction

A strong easterly wind current associated with the Hadley circulation is predominant throughout the year over the Caribbean Sea. Wind speeds around the 925 hPa level peak twice a year, during February and July. This low-level wind current exhibits a semiannual cycle extensively reported in previous studies [Amador, 1998, Amador et al., 2003, 2006; Wang, 2007; Amador, 2008; Muñoz et al., 2008; Whyte et al., 2008; Cook and Vizy, 2010; Maldonado et al., 2016a]. In the literature this wind current is often known as the Caribbean low-level jet (CLLJ). Previous studies such as Amador [2008] and Cook and Vizy [2010] show strong evidence that both the structure and dynamical mechanisms involved in the formation and weakening of the CLLJ are not necessarily the same during February and July and that the processes controlling the CLLJ remain, to a large extent, unknown [Amador, 2008].

The CLLJ exerts an important influence on convective activity in the Central American and Caribbean regions, during the summer months (June–September). The interaction with other features such as easterly waves [Amador, 1998, 2008] and the western hemisphere warm pools [Wang and Enfield, 2001] controls the formation of deep convection, i.e., convective activity over the Caribbean Sea and the Pacific side of Central America is weakened (intensified) when the CLLJ is stronger (weaker) [Amador, 2008]. This control occurs in different ways: on the one hand, the CLLJ is known to be the main driver of the vertical wind shear over the Caribbean Sea, which is a region of high tropical cyclogenesis; therefore, there exists a strong relationship between the CLLJ and the hurricane activity [Amador et al., 2006; Wang and Lee, 2007; Amador, 2008; Amador et al., 2010]. In addition, the CLLJ is the main moisture transport mechanism from the Caribbean to different regions in the American continent [Durán-Quesada et al., 2010, Gimeno et al., 2016], including Central America, the Gulf of Mexico, and southern United States of America. The CLLJ is also a supplier of moisture

for the American monsoon systems [Amador *et al.*, 2006; Vera *et al.*, 2006; Amador, 2008]. On the other hand, Herrera *et al.* [2015] pointed out that the CLLJ is also the main cause of the marked reduction in precipitation during July and August over Central America, known as the midsummer drought (MSD) [Magaña *et al.*, 1999; Amador *et al.*, 2006; Amador, 2008], and the increase of rainfall during the same season in the Caribbean side of Central America, due to convergence at the jet exit [Amador, 2008].

In February, the relationship of the CLLJ with the deep convection activity is not completely known [Amador *et al.*, 2006; Amador, 2008]. Recently, it has been reported that the CLLJ interacts with cold air outbreaks from the Northern Hemisphere [Zárate-Hernández, 2013, 2014; Maldonado *et al.*, 2016a], thus connecting the CLLJ with the main mechanism controlling rainfall during February in the Caribbean coast of Central America [Zárate-Hernández, 2013, 2014]. Other less frequent cloud systems traveling from the east [Velásquez, 2000] cause rainfall during February; nevertheless, their connection with the CLLJ is still not clear. Furthermore, the CLLJ has been shown to affect the hydrological cycle during spring in the central and southern United States of America, due to its relationship with tornadic activity and precipitation throughout the southeasterly wind shear, dry transients at the midtroposphere, moist transients at low levels, and an increase in convective available potential energy [Muñoz and Enfield, 2011]. Considering the importance of the CLLJ for the climate and weather in the above mentioned regions, the understanding of the mechanisms controlling the structure and development of the CLLJ is vital to improve our knowledge of the atmospheric dynamics in the Caribbean region and to develop an integrated prediction system of precipitation for February and July in Central America.

In an attempt to explain the observed vertical structure and the origin of the CLLJ, several studies [Wang, 2007; Muñoz *et al.*, 2008; Cook and Vizy, 2010] have pointed to the existence of strong meridional surface temperature gradients related to the jet in the Caribbean basin. A northward sea surface temperature (SST) gradient develops contrary to a southward air temperature gradient close to the mountains, due to the land-sea contrasts between the Caribbean Sea and Northern South America (NSA) [Muñoz *et al.*, 2008]. Wang [2007], used the conceptual model of Lindzen and Nigam [1987] to propose that a well-defined northward meridional SST gradient during both February and July is coupled with the atmospheric boundary layer (ABL) through vertical mixing and induces a meridional sea level pressure (SLP) gradient over the Caribbean Sea, which—in addition to the seasonal migration of the North Atlantic Subtropical High (NASH)—can intensify the CLLJ. Such a hypothesis, however, fails to explain the seasonal variations in intensity and vertical structure of the CLLJ: i.e., the CLLJ is stronger in July than in winter, having in February a more confined vertical structure, while the SST gradient instead is stronger in February than in July [Amador, 2008]. In a recent study, however, Chang and Oey [2013] support the idea of the SST-CLLJ coupling. They pointed out the existence of the coupling between the meridional SST gradient in the Caribbean and the trade winds from seasonal and interannual to decadal scales. Chang and Oey [2013] also showed that the SST gradient anomalies are caused by a variation in the strength of coastal upwelling by the wind, which in turn strengthens (weakens) due to a stronger (weaker) SST gradient.

In addition, Muñoz *et al.* [2008] proposed a baroclinic structure of the CLLJ, due to the above mentioned southward air temperature gradient produced by the sea-land temperature contrast. They also suggested that the horizontal jet structure is a consequence of the wind interaction with the mountains over Greater Antilles and NSA through a funnel effect. Cook and Vizy [2010] observed that in boreal February the meridional geopotential gradient is mainly modulated by the warming of the NSA edge. This warming results in an intensification of the meridional geopotential gradient that accelerates the CLLJ due to the geostrophic balance.

Some of these hypotheses about the jet structure and formation have been challenged. For example, Ranjha *et al.* [2013] found that the CLLJ is not related to the land-sea thermal contrast. In their study, Ranjha *et al.* made a global classification of coastal low-level jets using the ERA-Interim reanalysis [Dee *et al.*, 2011]. In this classification, a coastal low-level jet is produced basically due to the land-sea temperature contrast. Ranjha *et al.*'s algorithm, however, fails to detect the CLLJ. They argue that this failure occurs because the CLLJ is not related to land-sea thermal contrasts. However, based on previous studies such as Wang [2007], Ranjha *et al.* suggest that this result is, instead, related to the SST in the Caribbean. Moreover, studies such as Molinari *et al.* [1997], Amador [1998, 2008], and Salinas-Prieto [2006] have reported the Caribbean region as barotropically unstable in July that could allow, under appropriate conditions for the mean flow, to

Table 1. Description of the Experiments Carried Out With the Atmospheric Model IFS Part of EC-EARTH Consortium^a

Experiment ID	Test
CR01	Unmodified SST monthly means
EX01	12 monthly climatological SST (1990–2004)
EX02	Same SST data as in the CR01, but the meridional SST gradient in the area 10°–17.5°N, 60°–83°W (D01) is removed (decreased).
EX03	Mountains in the area in NSA (approximately 8.5°–11.5°N, 66°–75°W, D02) are flattened. Unmodified SST data are used.

^aThe model resolution is TL255L91 (approximately 80 km and 91 vertical levels). Every simulation is run for the 15 year period 1990–2004.

exchange kinetic energy with the easterly waves and other transients resulting in acceleration (or deceleration) of the CLLJ.

Atmospheric models can provide relevant information about the dynamical mechanism involved in the structure, formation, and decay of the CLLJ. The representation of the CLLJ in general circulation models, however, is currently a challenge. In general, models have the ability to simulate the location and height of the CLLJ; however, the observed semiannual cycle of the CLLJ magnitude was a challenge for the models to reproduce. In particular, model means failed to capture the strong July CLLJ peak as a result of the lack of westward and southward expansion of the NASH between May and July [Martin and Schumacher, 2011]. However, Hidalgo and Alfaro [2015] reported that some models (including the EC-EARTH) skillfully reproduced the seasonal distribution of the CLLJ.

In this study, we aim to improve understanding of the role played by the SST gradient and topography in governing the CLLJ and their contribution to variations of SLP and precipitation over Central America by examining the baroclinic structure of the CLLJ by means of an atmospheric model. We have designed a set of three experiments to explore the impact of the meridional SST gradient and the topography in NSA on the vertical structure of the CLLJ. The article is structured as follows: data sets, atmospheric model, and experimental design are described in section 2 and a summary of the main results is shown in section 3. In section 4 an alternative approach to understand the CLLJ structure is presented. The discussion and conclusions are presented in section 5.

2. Data, Model, and Experimental Setup

2.1. Reanalysis

We validate the model outputs with ERA-Interim reanalysis [Dee et al., 2011] monthly means products of SLP, horizontal wind at 925 hPa, and precipitation. The spatial resolution of the data set is approximately 80 km (T255 spectral) on 60 vertical levels from the surface up to 0.1 hPa. The averages are estimated for the simulated the period January 1990 to December 2004. The study period contains four El Niño (1991–1992, 1994–1995, 1997–1998, and 2002–2003) and four La Niña (1995–1996, 1998–1999, 1999–2000, and 2000–2001) events, according to the Oceanic El Niño index [National Oceanic and Atmospheric Administration, 2016]. The meridional SLP gradient and SLP area average are calculated for the area bounded by 12.5°–17.5°N and 70°–80°W, whereas for the horizontal wind and precipitation we used the region enclosed by 7°–20°N and 75°–95°W to estimate the climatology.

2.2. Atmospheric Model

The Integrated Forecast System (IFS, branch 36r4) atmospheric model, provided by the EC-EARTH consortium (<http://www.ec-earth.org/>) and developed by the European Centre for Medium-Range Weather Forecasts (ECMWF, <http://www.ecmwf.int/>), is used to carry out the experiments. The model is configured with a T255L91 resolution which is approximately 80 km of horizontal resolution and 91 vertical levels. The outputs are set to 16 levels below the 500 hPa. Aerosols interactions are turned off due to stability issues present in the used version of IFS. Since the focus of this study is on the dynamics, the removal of this interaction is not expected to have a significant impact on the final results.

2.3. Experimental Design

We design a set of three experiments to study the impact of the meridional SST gradient in the Caribbean Sea and the topography in NSA on the vertical structure of the CLLJ during February and July (Table 1). The SST

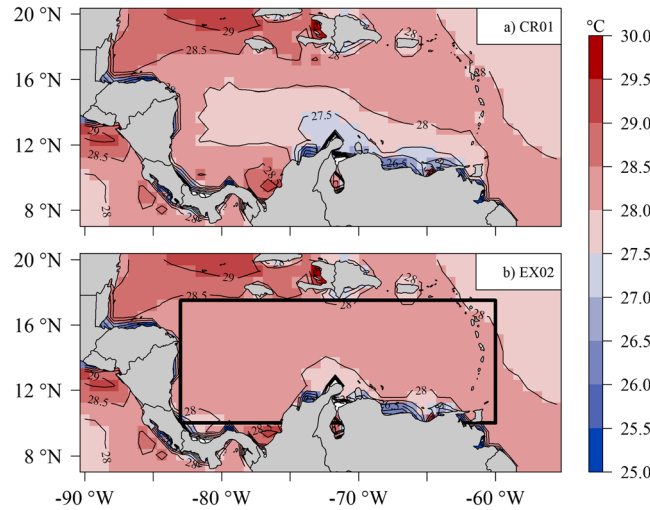


Figure 1. To illustrate the differences among the simulations described in section 2.3 and in Table 1, here is shown the July climatology for 1990–2004 period of the sea surface temperature (SST, °C) used as prescribed boundary conditions for the atmospheric model in the simulations. (a) Unmodified meridional SST 15 year climatology used in CR01, EX01, and EX03. (b) The modified July SST 15 year climatology (without meridional SST gradient over the Caribbean Sea) in EX02. The contour lines and color shades are spaced every 0.5°C. The box represents the area where the meridional SST gradient has been modified (10°–17.5°N, 60°–83°W, D01).

(EX02), the original SST is modified over the area 10°–17.5°N, 60°–83°W (D01) in order to remove the influence of the meridional SST gradient. Figure 1b shows the July SST 15 year climatology over the Caribbean Sea used in this experiment. The gradient is almost suppressed using an interpolation method based on invert-distance weighted smoothing. The boundaries to perform such interpolation are located between the east and west limits of D01 (i.e., 60° and 83° meridian), where the meridional gradient is less intense. The meridional SST and SLP gradients are calculated as the latitudinal differential change between 10° and 17°N, over the same longitude, i.e., the gradients are

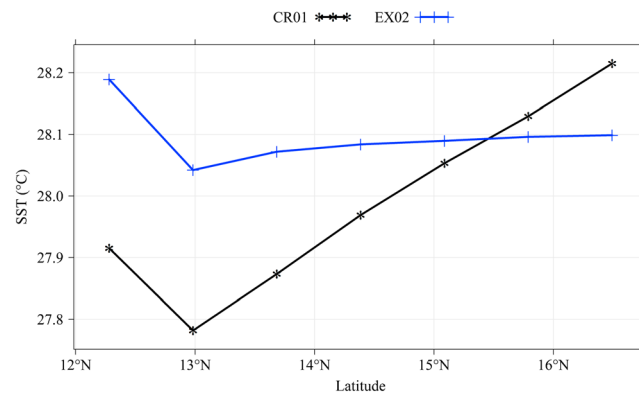


Figure 2. North-south transect of July climatology for 1990–2004 period of the sea surface temperature (SST) monthly mean over the domain 10°–17.5°N, 60°–83°W (D01). The transect is calculated for each of the cases shown in Figure 1, i.e., the CR01 (black line), and EX02 (blue line). Note that the black line is also representative EX01 and EX03. The north-south transect is the SST zonal average between 60° and 83°W.

data set to force the atmospheric model is the same SST analysis used as prescribed boundary conditions for the atmospheric model in ERA-Interim project [Dee et al., 2011].

Every simulation is run for the period 1990–2004. In the control run (CR01) we force the atmospheric model with unmodified SST analysis. The first sensitivity experiment (EX01) is carried out using the climatological SST calculated for the 1990–2004 period, that is, the model is forced with only 12 monthly climatology of SST for the 15 year simulation. The aim of running an experiment using climatological SST is to remove the effects of variability sources such as El Niño–Southern Oscillation (ENSO), i.e., the 3–4 years interannual variability, and to compare the difference between the simulations with and without such variability sources. The July SST 15 year climatology for these two simulations is shown in Figure 1a.

In the second sensitivity experiment (EX02), the original SST is modified over the area 10°–17.5°N, 60°–83°W (D01) in order to remove the influence of the meridional SST gradient. Figure 1b shows the July SST 15 year climatology over the Caribbean Sea used in this experiment. The gradient is almost suppressed using an interpolation method based on invert-distance weighted smoothing. The boundaries to perform such interpolation are located between the east and west limits of D01 (i.e., 60° and 83° meridian), where the meridional gradient is less intense. The meridional SST and SLP gradients are calculated as the latitudinal differential change between 10° and 17°N, over the same longitude, i.e., the gradients are estimated approximating with finite differences the partial derivative $\partial X/\partial y$, where X is the field (SST or SLP) and ∂y is the distance between two points of the grid. Then, the result is averaged for all the longitudes within the area enclosed by 83°–63°W. Figure 2 shows the north-south transect over the region where the SST is changed, to illustrate the meridional SST gradient across the latitudes. In CR01 (EX01 and EX03) the increase in the SST from 13°N toward north is about 0.4°C, while in EX02 the SST is almost constant. Figure 2 also indicates that the gradient was reduced 1 order of magnitude ($\sim 1 \times 10^{-7}$ C/m), compared to the unmodified SST in this case. A noticeable remark is that in average, using a two-sided Kolmogorov-Smirnov test for comparison, the

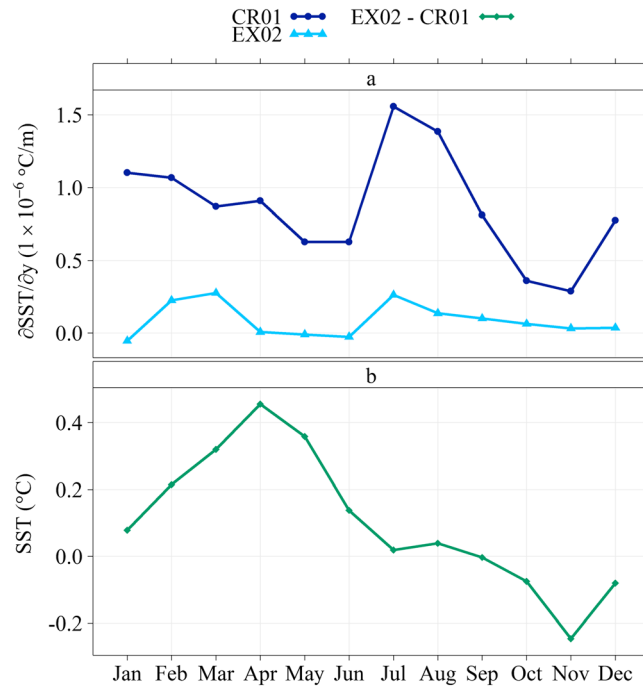


Figure 3. Annual cycle of the (a) meridional sea surface temperature (SST) gradients and (b) difference of the area average of SST in the region bounded by 10°–17.5°N, 60°–83°W (D01) for the CR01 and experiment EX02. The difference is computed as EX02 minus CR01. The meridional gradients are calculated as the latitudinal differential change between 10° and 17°N, over the same longitude. Then, the result is averaged for all the longitudes within the area enclosed by 83°–63°W. The SST area average is estimated for the same region.

meridional SST gradient is decreased significantly (1% test level) compared to the unmodified SST (Figure 3a); however, the annual cycle of the SST remains similar, with a slight increase (approximately 0.4°C maximum) of the temperatures mainly during April–May of the year (Figure 3b). An increment of this magnitude in the SST over this region has been shown to generated perturbations in the vertical structure of the troposphere upon the Caribbean Sea and tropical North Atlantic (TNA) that can be related with the formation of rainfall systems, and so, wetter conditions during the early rainy season in the Caribbean Sea and Central America [Knaff, 1997; Chen and Taylor, 2002; Maldonado et al., 2016b].

The influence of topography is tested in the third sensitivity experiment (EX03), where the orography is manipulated in order to reduce the height of the mountains in NSA (approximately 8.5°–11.5°N, 66°–75°W, D02, Figure 4). The reduction of the terrain heights is done using the same methodology to reduce the SST gradient in EX02. In EX03 the SST input to

force the model is the same as in the CR01. The mountains with heights around 1000–1500 m are decreased to approximately 200 m heights in the input terrain data. This configuration is expected to have a twofold impact: first, the funnel effect should be minimized, leading to a possible reduction in the wind intensity, and second the geopotential heights should change reducing the meridional gradient, and so, weakening the CLLJ.

The time series for the variables of interest (e.g., SLP) from reanalysis versus CR01, and from experiments versus the control run, are compared using two-sided Kolmogorov-Smirnov test to see if they come from the same distribution. Using this test, it can be determined if the differences among the results are significant or not.

3. Results

3.1. Sea Level Pressure and Caribbean Low-Level Jet

In order to examine the structure of the CLLJ, we calculated the area-averaged SLP, the meridional SLP gradient, and the zonal wind at the 925 hPa, level, over the region bounded by 12.5°–17.5°N and 70°–80°W, where the jet core is located. The SLP estimated in ERA-Interim reproduce a semiannual cycle previously reported by Wang [2007], with SLP peaking in February and July (Figure 5a). This seasonality is attributed to the seasonal migration of the NASH. To validate the model, the CR01 is compared against reanalysis. CR01 also shows the bimodal cycle in the SLP; nonetheless, it is underestimated when compared to reanalysis (p value = 0.26, the difference is not significant to the 0.05%). The SLP semiannual cycle is also visible in all the three experiments. EX01 shows higher SLP values than the rest of experiments for the 12 months. However, EX01 is lower than reanalysis from January to April and higher than reanalysis the rest of the year. The experiments against the control run have a p value > 0.05%; the differences are not significant.

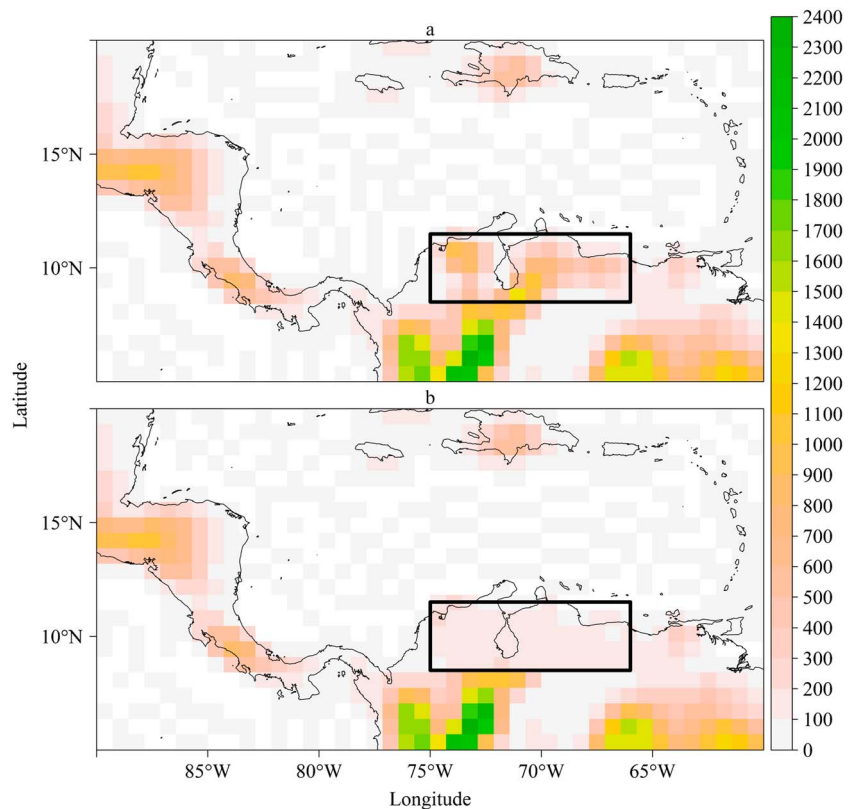


Figure 4. Terrain setup used in (a) CR01 and in (b) experiment EX03. The black box shows the mountains over northern South America (NSA, approximately 8.5°–11.5°N, 66°–75°W), where the terrain has been partially decreased in EX03 from height around 1200–1500 m to 200 m. Color shades show the terrain height in meters above sea level.

The meridional SLP gradient (Figure 5b) and the zonal wind (Figure 5c) also show the same seasonality noted for the mean SLP in reanalysis and all the simulations. CR01 overestimates the meridional SLP gradient compared to reanalysis (significant to the 0.05% test level). Note that the results from the experiments are more scattered from January to June, while during July–December the curves have better agreement when compared with CR01. However, the difference between the curves is not significant to the 0.05%. The same scattering is noticeable for the zonal wind; however, the differences between reanalysis and the control run are not significant, neither among the experiments to the 0.05%.

However, one could speculate about the causes of the discrepancies found from January to June. First, the differences detected from January to June may be related to intrarun variability of the model. There are also physical mechanisms that occur during this period that can be interfering somehow in the simulations. During February and spring, the pressure field can be perturbed by different synoptic elements affecting the Caribbean region, i.e., cold surges [Zárate-Hernández, 2013, 2014], the NASH is weak and located farther west [Wang, 2007], and ENSO influence is strong during the beginning of the year in the North Atlantic [Wang, 2007; Amador, 2008]. Furthermore, errors related to the model representation of these elements might be involved in each simulation [Martin and Schumacher, 2011].

The peaks in the SLP and meridional SLP gradient coincide with the maxima in the CLLJ in July and the minima of SLP and the gradient with the lowest value of the CLLJ in October. According to Wang [2007], the meridional SST gradient in this region is coupled with the ABL in such a way that it can induce the observed meridional SLP gradient associated to the CLLJ. The results from the sensitivity experiment (EX02), however, in which the meridional SST gradient over the Caribbean Sea is significantly decreased (almost removed), suggest that the model is not capturing the possible feedback from the SST to the ABL over the Caribbean Sea, thus discarding any coupling between the SST and the ABL as previously

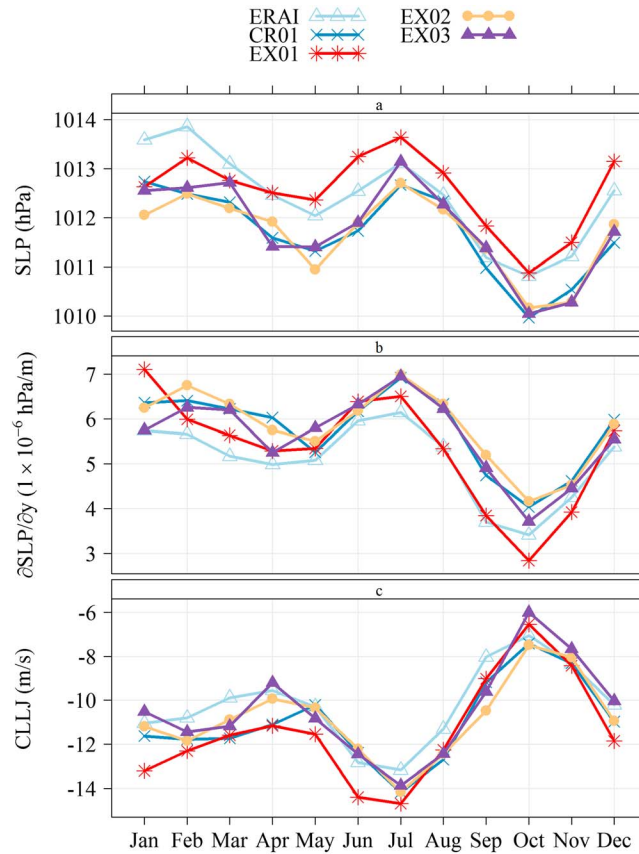


Figure 5. Annual cycle of the (a) mean sea level pressure (SLP), (b) meridional SLP gradient, and (c) zonal wind at 925 hPa, in the area bounded by 12.5°–7.5°N and 70°–80°W for the ERA-Interim reanalysis, the CR01, and the sensitivity experiments (EX01 to EX03). The meridional SLP gradient is calculated in the same way than the meridional sea surface temperature (SST) gradient described in Figure 3 but for the region mentioned in this description.

funnel effect and controlling mechanisms of the meridional geopotential gradient. The latter, however, should be taken with caution, since in EX03 the model might experience problems related to imbalance in the pressure field, due to the changes in the terrain.

The monthly time series for the zonal wind and the meridional SLP gradient show comparable interannual variability among the experiments (Figures 6a–6e), i.e., the wavelet transform locates most of the energy in periods of about 4 to 8 years (not shown) in both time series, and it can be related to ENSO events [Wang, 2007]. Despite the modifications of the SST gradient (Figures 6c and 6d), the meridional SLP gradient and the CLLJ are still present. The cross-wavelet coherence (not shown) between the time series of the latitudinal gradient of SST (SLP) and the zonal wind show that the changes of the SST in the Caribbean are strongly related to anomalies in both the meridional SLP gradient and the CLLJ. The latter shows again the possible one-way coupling between the SST and the CLLJ [Amador, 2008; Chang and Oey, 2013].

We also compare the changes in the horizontal and vertical structure of the wind, under the modifications in the experiments set. The presence of the CLLJ is noticeable in all simulations during February and July, as shown in Figure 7. The differences between each experiment and the control run are close to zero in the vicinity of the jet core. However, in February (Figures 7a, 7c, and 7e) the difference increases near 18°–20°N. During this month, as mentioned above, synoptic processes can produce fluctuations in the pressure field and so in the wind. Higher differences are found in Figure 7a, which corresponds to EX01. These results show that by removing the 3–4 year interannual variability, the effect is to increase the wind at low levels over

hypothesized by Wang [2007]. Despite that the meridional SST gradient is reduced (also increased and/or constant in the same region, not shown), the bimodal cycle in the meridional SLP gradient, and in the CLLJ, is still reproduced by the model. This result suggests that the meridional SST gradient is not the main driver for the latitudinal gradient in SLP. Nevertheless, this outcome does not rule-out the possible one-way coupling through Ekman mechanics between the low-level wind and the SST over the Caribbean Sea that can produce, intensify, and modulate the meridional SST gradient over this sea [Amador, 2008; Chang and Oey, 2013].

The results of the experiment EX02 strongly suggest that the meridional SST gradient alone is not sufficient to explain the jet vertical structure, contrary to what has been previously suggested by Wang [2007]. Moreover, the results from EX03 show that the model is also not sensitive to changes in the height of the mountains in NSA. Hence, our results do not support also the hypotheses brought forward by Muñoz *et al.* [2008] and Cook and Vizy [2010] on the influence of the mountains on the CLLJ's core strength through

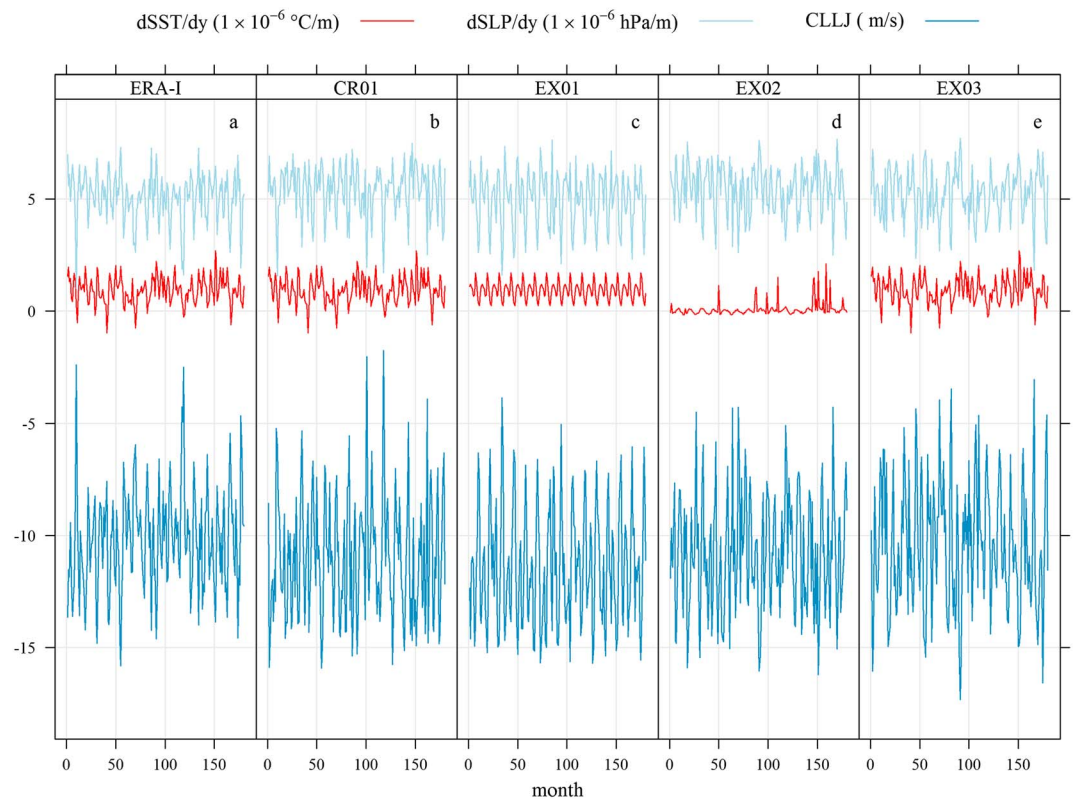


Figure 6. Monthly time series of the area average in the region bounded by 12.5°–17.5°N, 70°–80°W, for the meridional gradients of sea surface temperature (SST, red lines) and sea level pressure (SLP, light blue lines) and the zonal wind at 925 hPa (dark blue lines). The time series were calculated using data from (a) ERA-Interim reanalysis (ERA-I), (b) CR01, (c) EX01, (d) EX02, and (e) EX03. The meridional gradients are calculated in the same way than in Figure 3 but for the area in this description.

18°–20°N. The impact of ENSO events on the wind over the same region during February has been already studied by *Maldonado et al.* [2016a]. These authors found that the signal of ENSO episodes in the SLP over the eastern coast of United States changes the circulation patterns of the wind, mainly in the northern part of the Caribbean Sea and the Gulf of Mexico.

EX03 (Figures 7e and 7f) shows an increment of the horizontal wind in the northern part of South America, where the mountains were reduced (D02), yet the wind over the jet core region does not show remarkable changes. These results are also replicated in the vertical structure (Figures 8a–8f). The increase of the wind in NSA (8°–12°N, 70°–80°W) is likely due to the fact that by reducing the height of the mountains, we decrease a physical barrier for the wind, so it blows without any blocking in that region.

Furthermore, we estimate the thermal wind using the geopotential height gradients as in *Holton* [2004] for each experiment. The thermal wind from EX01 and EX02 do not shown any remarkable differences; therefore, the results for those experiments are not shown. In EX03, however, the thermal wind relation shows that over the D02 at low level the thermal wind has an easterly component that acts in favor of the mean flow (Figure 9). Another important change in the thermal wind relation is observed near 12°N. There, the thermal wind is reduced in EX03 compared to CR01; nonetheless, there is not a noticeable change in the CLLJ vertical structure (Figure 9).

3.2. Impact on Precipitation

In this section, we examine if precipitation anomalies are related with changes in the meridional SST gradient and topography, throughout variations of the CLLJ. The CR01 simulation underestimates precipitation over the western Caribbean Sea and Central America (7°–20°N; 95°–75°W) by at least 0.3 mm d⁻¹ in average per month compared to the ERA-Interim reanalysis (Figure 10), and this difference (significant at the 0.10% test

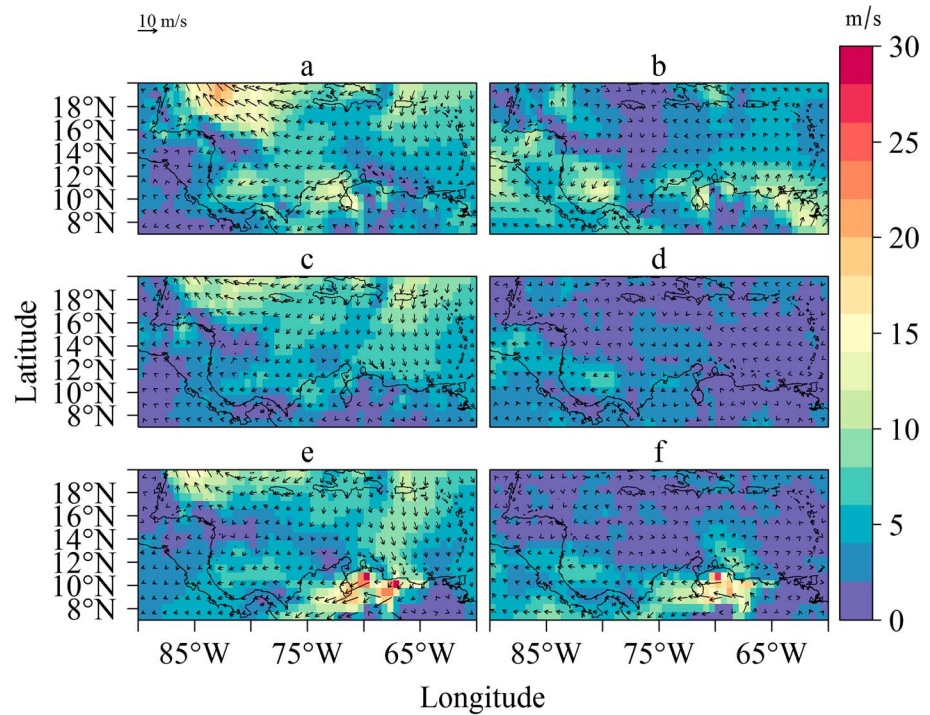


Figure 7. Monthly mean differences for (a, c, and e) February and (b, d, and f) July of horizontal wind at 925 hPa from EX01-CR01 (Figures 7a and 7b), EX02-CR01 (Figures 7c and 7d), and EX03-CR01 (Figures 7e and 7f). The shadings show the absolute value of the wind speed difference in m s^{-1} , and the arrows show the wind direction fluctuation and are proportional to the wind speed anomaly.

level) is larger in the months following June. The precipitation in every experiment is similar to CR01, except from May to July where the EX01 and EX03 display greater rainfall up to 0.5 mm d^{-1} compared to the CR01. These results from the experiments are not different at the 0.05% test level.

The MSD, however, is well developed in all experiments between July and August in agreement with reanalysis. These findings further corroborate the fact that both the meridional SST gradient over the Caribbean Sea and the mountains over the NSA edge have minor impact on the precipitation over the Caribbean Sea in contrast to what was previously shown [Wang, 2007; Cook and Vizy, 2010, Chang and Oey, 2013]. The latter follows from the results that in none of the experiments the CLLJ has changed significantly to impact the moisture transport, and the vertical wind shear, which are known to be related with rainfall production in the region, resulting in modifications of the hydrological cycle. It seems coherent as the results also show no influence on the strength or annual cycle of the CLLJ, assuming that the CLLJ and the precipitation over the Caribbean seem to be related as shown by previous study. These results thus do not suppress the idea that the rainfall over Central America and the CLLJ are related (stronger CLLJ and larger amount of precipitation over the Caribbean side of Central America) and that the CLLJ could force the meridional SST gradient explaining why both show the annual cycle.

The discrepancies found in precipitation among the simulations might arise due to the fact that the rainfall area average includes regions located in both the Pacific and Caribbean basins, and the annual cycle of precipitation in these areas is not necessarily the same. Other differences may be also related to the sensitivity of the model to ENSO, i.e., in the simulation EX01, the ENSO influence is suppressed; therefore, the results might vary in comparison to the CR01, EX02, and EX03, where the ENSO signal is present. It is worth saying that in EX02, the area average of the SST over the Caribbean Sea was increased about 0.5°C during May–June in comparison to the climatology. From the results of Maldonado et al. [2016b], wetter conditions might therefore be expected during the early rainy season in Central America and the Caribbean Sea for EX02. Precipitation during May–June in EX02 is, however, of the same order of magnitude than the control run with one possible reason being that the SST anomalies associated with precipitation anomalies during these months, as

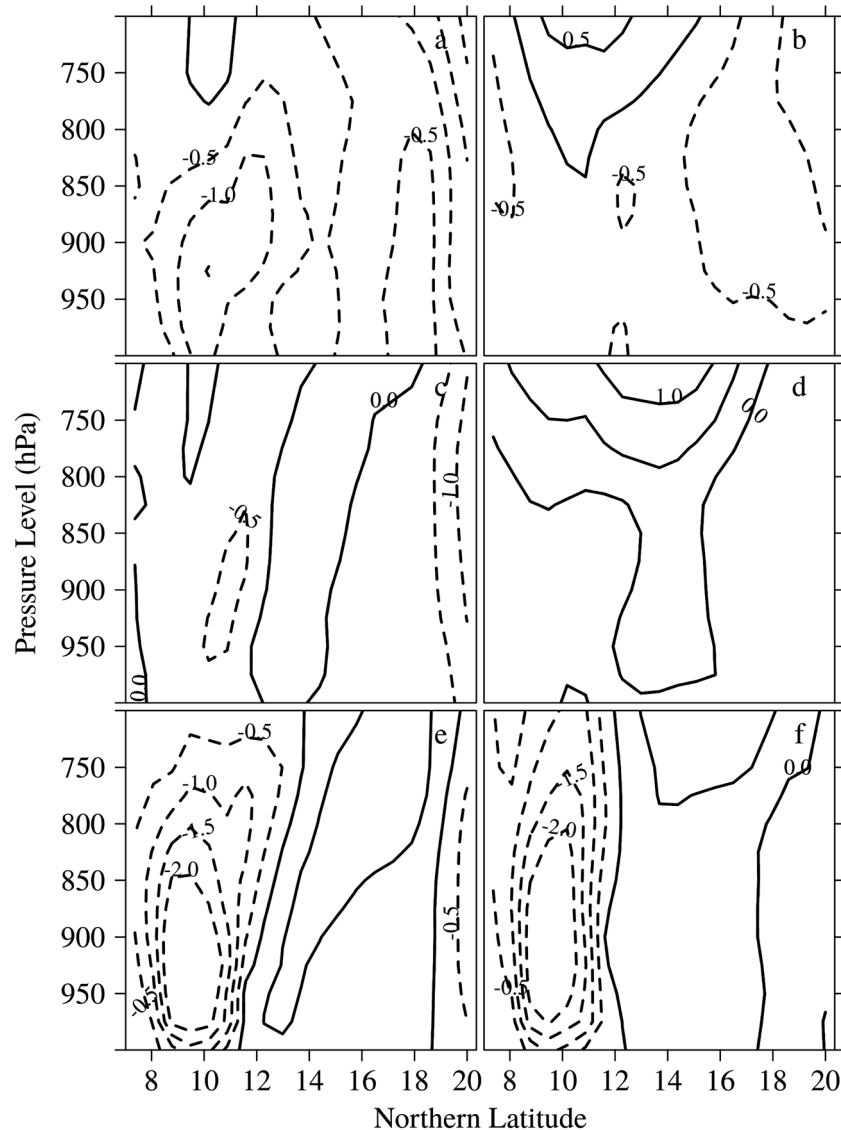


Figure 8. Monthly mean differences for (a, c, and e) February and (b, d, and f) July of the pressure-latitude cross section of the zonal wind between 70° and 80°W from EX01-CR01 (Figures 8a and 8b), EX02-CR01 (Figures 8c and 8d), and EX03-CR01 (Figures 8e and 8f). Dashed (solid) line contours show negative (positive) anomaly values. The contours are spaced each 0.5 m s⁻¹.

reported by *Maldonado et al.* [2016b] were focused over the TNA region rather than in the Caribbean Sea as in our case.

4. Barotropic Structure of the CLLJ

In this section, an alternative approach to understand the dynamics governing the structure of the CLLJ is presented. The hypothesis is based in the concepts previously outlined by *Amador* [1998], *Salinas-Prieto* [2006], *Amador et al.* [2006], and *Amador* [2008] related to the barotropic unstable conditions present over the Caribbean Sea year-round. Furthermore, only results from reanalysis are shown, since the simulations show agreement with reanalysis in representing the dynamical variables studied in this work.

In most of the literature the authors have tried to explain the CLLJ vertical structure and so the vertical wind shear using a baroclinic structure due to the surface temperature latitudinal gradients over the Caribbean Sea [e.g., *Wang*, 2007; *Muñoz et al.*, 2008], obviating the horizontal shear also present when the jet peaks. However, in the previous section it was found evidence that such a hypothesis does not explain the actual

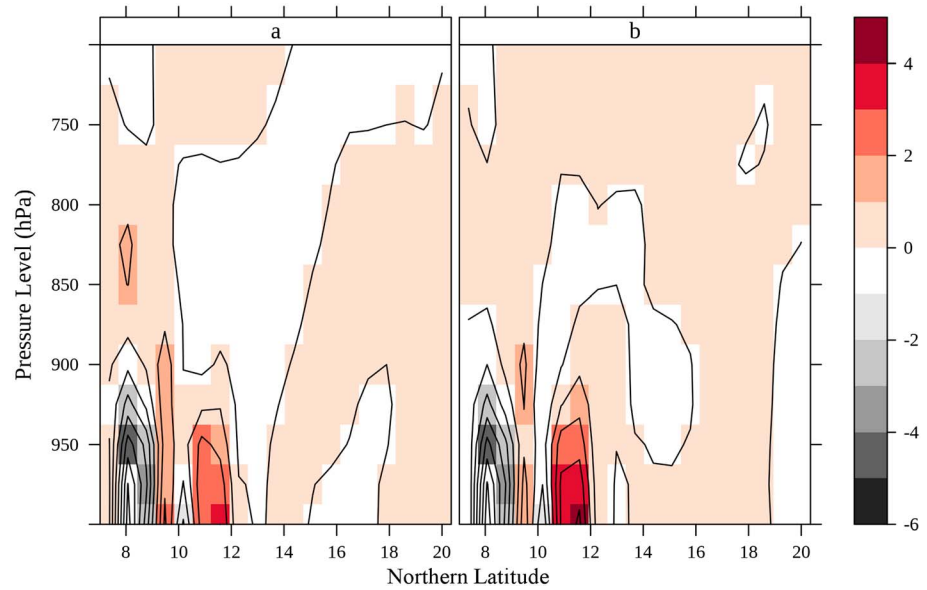


Figure 9. Pressure-latitude cross-section differences of EX03 minus CR01 calculated for the zonal average between 70° and 80°W for the zonal component of the thermal wind (m s^{-1}) for (a) February and (b) July.

structure of the CLLJ. Another important feature highlighted in the literature is the fact that the wind is considered to be in geostrophic balance and therefore discarding the ageostrophic component, despite the proximity to the equator. The latter is not a proper approximation as shown in Figure 11. In this figure the actual zonal wind is compared with the geostrophic zonal component. The geostrophic wind is estimated using the geopotential and the approximation $U_g = -\frac{1}{f} \frac{\partial \Phi}{\partial y}$, and $V_g = \frac{1}{f} \frac{\partial \Phi}{\partial x}$, where U_g and V_g are the zonal and meridional components of the geostrophic wind, f is the Coriolis parameter, and Φ the geopotential. From here, it is seen that the vertical shear of the actual wind cannot be explained by the vertical shear of its geostrophic zonal component. Conversely, the horizontal shear of the actual wind follows the horizontal shear of the geostrophic component of the wind.

Moreover, the CLLJ vertical structure must be explained then by the interaction of the friction forces at the surface layer. Figure 12 shows the ageostrophic component of the horizontal wind below the jet core (1000 hPa). This component is to the right of the friction force, showing a cross-isobaric flow from high to low pressure. Therefore, this result suggests the importance of including the Coriolis and friction forces as was also noted by Cook and Vizy [2010], to get a complete understanding of the dynamics involve in the structure of the CLLJ.

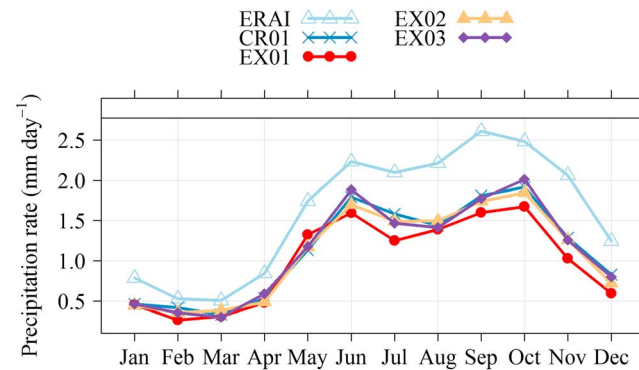


Figure 10. Annual total precipitation cycle (mm d^{-1}) in the area bounded by 7°–20°N and 75°–95°W. This figure shows a comparison among ERA-Interim reanalysis (ERA-I), CR01, and the experiments (EX01 to EX03).

5. Discussion and Conclusion

Previous work that focused on the climate dynamics in the Caribbean region has suggested that the vertical structure of the CLLJ is a result of the SST latitudinal gradient within the basin [Wang, 2007]. In addition, both the horizontal and vertical structure of the jet have been related to topographic effects via interaction with the mountains in NSA, including funneling effects and the land-sea thermal contrast [Muñoz et al., 2008] and changes in the meridional geopotential height gradient due to

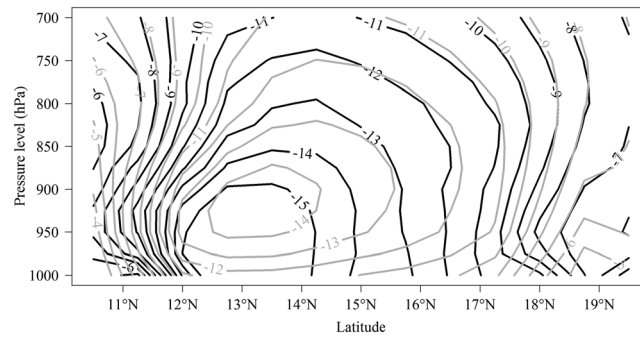


Figure 11. July monthly mean pressure-latitude cross section for the actual zonal wind (gray contours) and the geostrophic zonal component of the wind (black contours) from ERA-Interim reanalysis. Only the easterly component is shown. The average is estimated for the period 1990–2004. The cross section is estimated for the zonal average of the wind between 70° and 80°W.

the warming at the top of the mountains [Cook and Vizy, 2010].

In this study, we perform a set of idealized experiments using an atmospheric model to explore the contribution of the regional SST gradients and topography to the structure of the CLLJ. Our results show that the atmospheric model did a proper representation of important variables associated with the dynamics of the CLLJ and climate in Central America, such as the SLP and wind. The annual and seasonal cycles of fields such as pressure, wind, and precipitation show a bimodal structure in all the simulations comparable to reanalysis. This outcome can be related to

the fact that the SST area average over the Caribbean Sea did not change significantly in the simulations. The seasonal changes in the SST over the Caribbean Sea are influencing the rainfall and the tropical cyclone activity in association with other climate parameters such as the wind or the pressure. The regime of the rainfall is following the March season, and the higher amount of rainfall occurs when the SST are at their warmest in September–October. This is also when the tropical storm activity is intense. Inoue et al. [2002] also show that the cyclogenesis over the basin presents two peaks that correspond to the two peaks of rainfall observed for the Caribbean region.

Nevertheless, the model was not sensitive to the modification neither in the SST configurations used as prescribed boundary conditions nor the changes in the topography in NSA. The differences found in the representation of the mean fields of SLP, wind, and precipitation were statistically not significant. The annual and season cycles of these fields were not altered statistically speaking, under these modifications. Variability at interannual scales was also unaffected, with the exception of EX01 where the influence of ENSO was removed.

For these reasons, it can be argued that the meridional SST gradient over the Caribbean Sea is not the main element producing the jet's structure in that region. Our findings, however, do not discard the regional SST

gradient seasonal cycle as an important element for precipitation and tropical cyclone activity in the region [Wang and Enfield, 2001; Amador et al., 2006]. Our results also do not rule-out the one-way coupling between the low-level wind and the meridional SST gradient through friction forces as suggested in Amador et al. [2006] and Amador [2008].

Our findings do not support the possible influence on the CLLJ's vertical structure of the mountains over NSA through funnel effect or changes in the meridional geopotential height [Muñoz et al., 2008; Cook and Vizy, 2010]. These results, however, must be taken with caution, since in this case the model might be shown instability problems due to the imbalance of the pressure field related to changes in the terrain input.

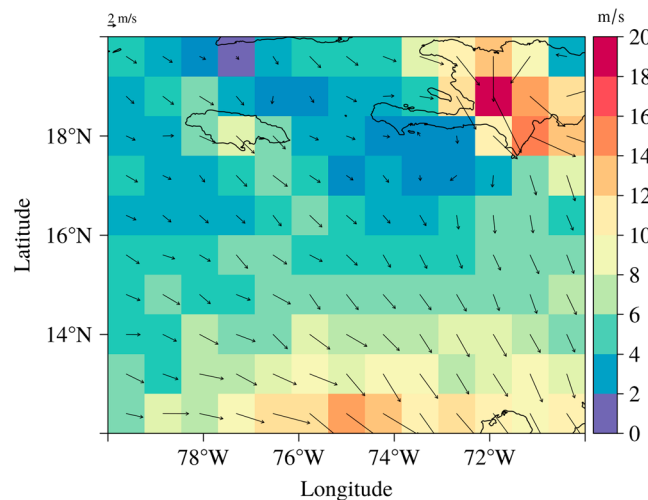


Figure 12. July monthly mean of the ageostrophic component of the horizontal wind at 1000 hPa from ERA-Interim reanalysis. The shadings show the wind speed ($m s^{-1}$), while the arrows represent the mean direction and the size is proportional to the wind speed.

These results are also reflecting the complexity of the dynamics governing the CLLJ intensity and vertical structure. Current hypothesis must be reviewed in order to fully understand the atmospheric dynamics over the Caribbean Sea. This study also highlights the relevance of high-resolution models to understanding dynamical processes that determine the climate in Central America. However, 80 km of horizontal resolution might be still coarse due to the heterogeneous geomorphological and meteorological features of Central America.

Acknowledgments

This research was carried out within the CNDS research school, supported by the Swedish International Development Cooperation Agency (SIDA) through their contract with the International Science Programme (ISP) at Uppsala University (contract 54100006). The authors would like to give special thanks to Klaus Wyser and Hamish Struthers and the Swedish National Infrastructure for Computing (SNIC) for their help and technical support. The model simulations were performed on resources provided by the Swedish National Infrastructure for Computing (SNIC) at the PDC Center for High Performance Computing at the KTH Royal Institute of Technology. The authors would like to thank also the 805-A9-532 (supported by CSUCA-ASDI) and 805-B6-143 (supported by Vice-presidency of Research at University of Costa Rica (UCR), CONICIT, and MICITT). All data for this paper are properly cited and referred to in the reference list.

References

- Amador, J. A. (1998), A climatic feature of the tropical Americas: The trade wind easterly jet, *Tóp. Meteorol. Oceanogr.*, *5*(2), 91–102.
- Amador, J. A. (2008), The intra-Americas sea low-level jet overview and future research, *Ann. N. Y. Acad. Sci.*, *1146*(1), 153–188, doi:10.1196/annals.1446.012.
- Amador, J. A., J. R. Chacón, and S. Laporte (2003), Climate and climate variability in the Arenal Basin of Costa Rica, in *Climate, Water and Transboundary Challenges in the Americas*, edited by H. Díaz and B. Morehouse, pp. 317–349, Kluwer Acad., Holland, Netherlands.
- Amador, J. A., E. J. Alfaro, O. G. Lizano, and V. O. Magaña (2006), Atmospheric forcing of the eastern tropical Pacific: A review, *Prog. Oceanogr.*, *69*(24), 101–142, doi:10.1016/j.pocean.2006.03.007.
- Amador, J. A., E. J. Alfaro, E. R. Rivera, and B. Calderón (2010), Climatic features and their relationship with tropical cyclones over the intra-Americas seas, in *Hurricanes and Climate Change*, vol. 2, pp. 149–173, Springer, Netherlands.
- Chang, Y. – L., and L.-Y. Oey (2013), Coupled response of the trade wind, SST gradient, and SST in the Caribbean Sea, and the potential impact on loop Lagrangian interannual variability, *J. Phys. Oceanogr.*, *43*(7), 1325–1344, doi:10.1175/JPO-D-12-0183.1.
- Chen, A. A., and T. A. Taylor (2002), Investigating the link between early season Caribbean rainfall and the El Niño +1 year, *Int. J. Climatol.*, *22*(1), 87–106, doi:10.1002/joc.711.
- Cook, K. H., and E. K. Vizi (2010), Hydrodynamics of the Caribbean low-level jet and its relationship to precipitation, *J. Clim.*, *23*(6), 1477–1494, doi:10.1175/2009JCLI3210.1.
- Dee, D. P., et al. (2011), The ERA-interim reanalysis: Configuration and performance of the data assimilation system, *Q. J. R. Meteorol. Soc.*, *137*(656), 553–597, doi:10.1002/qj.828.
- Durán-Quesada, A. M., L. Gimeno, J. A. Amador, and R. Nieto (2010), Moisture sources for central America: Identification of moisture sources using a Lagrangian analysis technique, *J. Geophys. Res.*, *115*, D05103, doi:10.1029/2009JD012455.
- Gimeno, L., F. Dominguez, R. Nieto, R. Trigo, A. Drumond, C. J. C. Reason, A. S. Taschetto, A. M. Ramos, R. Kumar, and J. Marengo (2016), Major mechanisms of atmospheric moisture transport and their role in extreme precipitation events, *Annu. Rev. Environ. Resour.*, *41*, 3.1–3.25, doi:10.1146/annurev-environ-110615-085558.
- Herrera, E., V. Magaña, and E. Caetano (2015), Air-sea interactions and dynamical processes associated with the midsummer drought, *Int. J. Climatol.*, *35*, 1569–1578, doi:10.1002/joc.4077.
- Hidalgo, H. G., and E. J. Alfaro (2015), Skill of CMIP5 climate models in reproducing 20th century basic climate features in Central America, *Int. J. Climatol.*, *35*, 3397–3421, doi:10.1002/joc.4216.
- Holton, J. R. (2004), *An Introduction to Dynamic Meteorology*, chap. 3, pp. 57–85, Academic Press, Burlington, Mass.
- Inoue, M., I. C. Handoh, and G. R. Bigg (2002), Bimodal distribution of tropical cyclogenesis in the Caribbean: Characteristics and environmental factors, *J. Clim.*, *15*, 2897–2905.
- Knaff, J. A. (1997), Implications of Summertime Sea level pressure anomalies in the tropical Atlantic region, *J. Clim.*, *10*, 789–804, doi:10.1175/1520-0442(1997)010<0789:IOSSLP>2.0.CO;2.
- Lindzen, R. S., and S. Nigam (1987), On the role of sea surface temperature gradient in forcing low-level winds and convergence in the tropics, *J. Atmos. Sci.*, *44*(17), 2418–2436, doi:10.1175/1520-0469(1987)044<2418:OTROSS>2.0.CO;2.
- Magaña, V., J. A. Amador, and S. Medina (1999), The midsummer drought over Mexico and Central America, *J. Clim.*, *12*(6), 1577–1588, doi:10.1175/1520-0442(1999)012<1577:TMDOMA>2.0.CO;2.
- Maldonado, T., A. Rutgersson, J. Amador, E. Alfaro, and B. Claremar (2016a), Variability of the Caribbean low-level jet during boreal winter: Large-scale forcings, *Int. J. Climatol.*, *36*(4), 1954–1969, doi:10.1002/joc.4472.
- Maldonado, T., E. Alfaro, A. Rutgersson, and J. Amador (2016b), The early rainy season in Central America: The role of the tropical North Atlantic SSTs, *Int. J. Climatol.*, doi:10.1002/joc.4958.
- Martin, E. L., and C. Schumacher (2011), The Caribbean low-level jet and its relationship with precipitation in IPCC AR4 models, *J. Clim.*, *24*, 5935–5950, doi:10.1175/JCLI-D-11-00134.1.
- Molinari, J., D. Knight, M. Dickinson, D. Vollaro, and S. Skubis (1997), Potential vorticity, easterly waves, and eastern Pacific tropical cyclogenesis, *Mon. Weather Rev.*, *125*(10), 2699–2708, doi:10.1175/1520-0493(1997)125<2699:PVEWAE>2.0.CO;2.
- Muñoz, E., and D. Enfield (2011), The boreal spring variability of the intra-Americas low-level jet and its relation with precipitation and tornadoes in the eastern United States, *Clim. Dyn.*, *36*(1), 247–259, doi:10.1007/s00382-009-0688-3.
- Muñoz, E., A. J. Busalacchi, S. Nigam, and A. Ruiz-Barradas (2008), Winter and summer structure of the Caribbean low-level jet, *J. Clim.*, *21*(6), 1260–1276, doi:10.1175/2007JCLI1855.1.
- National Oceanic and Atmospheric Administration (2016), National Weather Service, Climate Prediction Center. [Available at http://www.cpc.ncep.noaa.gov/products/analysis_monitoring/ensostuff/ensoyears.shtml].
- Ranjha, R., G. Svensson, M. Tjernström, and A. Semedo (2013), Global distribution and seasonal variability of coastal low-level jets derived from ERA-Interim reanalysis, *Tellus A*, *65*, doi:10.3402/tellusa.v65i0.20412.
- Salinas-Prieto, J. A. (2006), Dinámica de ondas del este y su interacción con el flujo medio en el Caribe, PhD thesis, Centro de Ciencias de la Atmósfera, Univ. Nacional Autónoma de México, México D.F., México.
- Vera, C., et al. (2006), Toward a unified view of the American monsoon systems, *J. Clim.*, *19*(20), 4977–5000, doi:10.1175/JCLI3896.1.
- Velásquez, R. C. (2000), Mecanismos físicos de variabilidad climática y eventos extremos en Venezuela, Tesis de Licenciatura en Meteorología, Departamento de Física Atmosférica, Oceánica y Planetaria, Escuela de Física, Universidad de Costa Rica, 118 pp. (Available at Biblioteca Central, Universidad de Costa Rica, 2060 San José, Costa Rica).
- Wang, C. (2007), Variability of the Caribbean low-level jet and its relations to climate, *Clim. Dyn.*, *29*(4), 411–422, doi:10.1007/s00382-007-0243-z.
- Wang, C., and D. B. Enfield (2001), The tropical western hemisphere warm pool, *Geophys. Res. Lett.*, *28*, 1635–1638, doi:10.1029/2000GL011763.

- Wang, C., and S.-K. Lee (2007), Atlantic warm pool, Caribbean low-level jet, and their potential impact on Atlantic hurricanes, *Geophys. Res. Lett.*, *34*, L02703, doi:10.1029/2006GL028579.
- Whyte, F. S., M. A. Taylor, T. S. Stephenson, and J. D. Campbell (2008), Features of the Caribbean low level jet, *Int. J. Climatol.*, *28*, 119–128, doi:10.1002/joc.1510.
- Zárate-Hernández, E. (2013), Climatología de masas invernales de aire frío que alcanzan Centroamérica y el Caribe y su relación con algunos índices árticos, *Tóp. Meteorol. Oceanogr.*, *12*(1), 35–55.
- Zárate-Hernández, E. (2014), Influencia de las masas invernales de aire frío sobre el Chorro de Bajo Nivel del Caribe y sus ramas, *Tóp. Meteorol. Oceanogr.*, *13*(2), 19–40.